Structural Engineering and Mechanics, *Vol. 49, No. 6 (2014) 793-810*
DOI: http://dx.doi.org/10.12989/sem.2014.49.6.793

A new finite element based on the strain approach with transverse shear effect

Mohammed Himeur*[1], Abdelaziz Benmarce[2a] and Mohamed Guenfoud[3b]

[1]*Department of Civil Engineering, Mentouri University, Constantine 25000, Algeria*
[2]*Department of Civil Engineering and Hydraulic, May 8, 1945 University, Guelma, 24000, Algeria*
[3]*Civil Engineering and Hydraulic Laboratory, Guelma University, 24000, Algeria*

(Received March 26, 2013, Revised December 24, 2013, Accepted February 1, 2014)

Abstract. This research work deals with the development of a new Triangular finite element for the linear analysis of plate bending with transverse shear effect. It is developed in perspective to building shell elements. The displacements field of the element has been developed by the use of the strain-based approach and it is based on the assumed independent functions for the various components of strain insofar as it is allowed by the compatibility equations. Its formulation uses also concepts related to the fourth fictitious node, the static condensation and analytic integration. It is based on the assumptions of tick plate's theory (Reissner-Mindlin theory). The element possesses three essential external degrees of freedom at each of the four nodes and satisfies the exact representation of the rigid body modes of displacements. As a result of this approach, a new bending plate finite element (Pep43) which is competitive, robust and efficient.

Keywords: finite elements; strain approach; static condensation; plate theory; Reissner-Mindlin

1. Introduction

Complex shell structures are frequently encountered in various fields. The development of simple and efficient finite elements for the analysis of these structures is a major thrust of scientific research in solid mechanics. Nevertheless, problems are often encountered, making difficult the achievement of the assigned objectives. Many finite elements are developed for solving these problems, but most of them have remained ineffective in the analysis of arbitrary geometric configuration. Isoperimetric elements are the most successful among those available in the literature due to their ability to successfully modeling curved structures. Only the phenomenon of shear locking leaves these elements unsuitable for the analysis of plates with distorted mesh. Despite the use of reduced integration and stabilization techniques of finite element in order to overcome this problem, the developed formulations did not converge to the solutions given by the theory of thin plates and often confront the problem of singularity of the stiffness matrix.

A brief review of the literature allows us to identify, but not limited, some recent work by

∗Corresponding author, Lecturer, E-mail: bet_himeur@yahoo.fr
[a]Assistant Professor
[b]Professor

http://www.techno-press.org/?journal=sem&subpage=8 ISSN: 1225-4568 (Print), 1598-6217 (Online)

researchers to address these problems:

• Development of a plate element by (Barik *et al*. 2002) that has the qualities of an element in terms of isoperimetric modeling capability with any mesh size, and without the disadvantage of the shear locking phenomenon.

• The amendments made by Chinosi (2005) at the boundary conditions for Reissner-Mindlin plates; prevent free boundary conditions to address the problem of convergence towards the reference solution for plates of small thickness.

• The triangular shell element with six nodes based on the approach MITC developed by (Do-Nyun *et al*. 2009) characterized by quality spatially isotopic element and the absence of zero energy modes.

The objective of this research is the formulation of shell finite elements based on the "strain approach" whose purpose is to overcome these difficulties on one hand, and the construction of finite shell elements which are simple and effective for the analysis of complex structures, on the other hand. To do this, we have enriched our approach with the concepts and development techniques based on the adoption of the "strain approach", the introduction of a "fictitious fourth node", the elimination of the degree of freedom corresponding to the "fictitious fourth node" by static condensation and the use of "analytic integration" to evaluate the stiffness matrix. Early works (Himeur 2008) led to the construction of triangular membrane finite elements which can be easily combined with inflected elements (slabs, beams and shells).

This ongoing work is a continuation for our research whose main focus this time is on the development of plate finite triangular elements. The new triangular finite element based on the strain approach for plate bending with transverse shear effect inflected with a fictitious fourth node the culmination of this above mentioned work. We call it «*Pep43*». This element is formulated by using the strain approach. The interpolation functions of the deformation fields' i.e., displacements and stresses are developed by using Pascal's triangle. It is a triangular element to which we added a fourth fictitious node positioned outside and away from the triangle. This position, outside, is thus chosen to avoid the relaxation of the stiffness matrix resulting in an overestimation of the nodal displacements. The degrees of freedom corresponding to the fourth node are then eliminated by the static condensation of the stiffness matrix at the elementary level. So the main interest of this fictitious node lies on the enrichment of the displacement field (*p* refinement i.e.: increase in the degree of the polynomial interpolation), which consequently leads to a greater precision in the approximation of the solution. The corresponding variational criterion is that of the total potential energy. The analytical integration for the evaluation of the stiffness matrix is highly interesting to avoid the loss of convergence phenomenon observed in isoperimetric elements which use numerical integration and are very sensitive (their convergence is conditioned by a regular mesh - undistorted). This formulation is based on the assumptions of the Reissner-Mindlin plate theory.

In an in order to validate the new «*Pep43*» element, we have undertaken a set of test cases. For each test case, the result is compared, on one hand, to the corresponding reference solution, and on the other hand, the solution is given by certain plate elements found in existing literature. On the whole, the approach in the present development has resulted in a competitive, robust and efficient «*Pep43*» plate finite element. This is visible, first, through its excellent convergence rhythm towards the reference solution, and secondly, through its behaviour performances towards other triangular plate elements in the existing literature: DKT, HCT (Batoz *et al*. 1990), C° (Belytschko 1984), ANST3 (Guenfoud 1990), ANST6 (Guenfoud 1990), TRUMP (Argyris *et al*. 1977) and SRI (Sabourin *et al*. 2000).

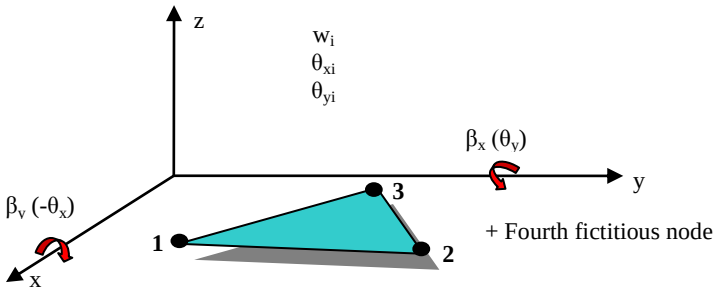

Fig. 1 Triangular plate element with *w*, *βx*, *βy* degrees of freedom each node

2. Basic equation of Reissner-Mindlin plate theory

2.1 Displacement field

In Fig. 1, the rotations around the two axes *x* and *y* are denoted θ_x and θ_y, and slopes in both directions are defined by the variables β_x and β_y with

$$\beta_x = \theta_y \qquad \beta_y = -\theta_x \tag{1}$$

Let the Reissner-Mindlin plate element shown in Fig. 1, be the field of displacements at any point in the Cartesian coordinate system, given by

$$w(x, y, z) = w(x, y)$$

$$u(x, y, z) = z\beta_x(x, y) = z\theta_y(x, y)$$

$$v(x, y, z) = z\beta_y(x, y) = -z\theta_x(x, y) \tag{2}$$

The infinitesimal strain tensor is thus

$$\varepsilon_x = \frac{\partial u}{\partial x} = z\frac{\partial \beta_x}{\partial x} \qquad \varepsilon_y = \frac{\partial v}{\partial y} = z\frac{\partial \beta_y}{\partial y} \qquad \gamma_{xy} = \frac{\partial u}{\partial y} + \frac{\partial v}{\partial x} = z\left(\frac{\partial \beta_x}{\partial y} + \frac{\partial \beta_y}{\partial x}\right)$$

$$\gamma_{xz} = \beta_x + \frac{\partial w}{\partial x} \quad \gamma_{yz} = \beta_y + \frac{\partial w}{\partial y} \tag{3}$$

The bending curvatures are given by equations

$$K_x = \frac{\partial \beta_x}{\partial x} \qquad K_y = \frac{\partial \beta_y}{\partial y} \qquad K_{xy} = \left(\frac{\partial \beta_x}{\partial y} + \frac{\partial \beta_y}{\partial x}\right) \tag{4}$$

2.2 Kinematics compatibility conditions

The kinematic compatibility conditions were established by St. Venant (1854) (Frey 1998). Their satisfaction is required to guarantee the uniqueness of the displacements. The compatibility equations are as developed as follows

$$\frac{\partial^2 K_x}{\partial y^2}+\frac{\partial^2 K_y}{\partial x^2}=\frac{\partial^2 K_{xy}}{\partial x\partial y}\quad ;\quad \frac{\partial^2 \gamma_{xz}}{\partial x\partial y}-\frac{\partial^2 \gamma_{yz}}{\partial x^2}+\frac{\partial K_{xy}}{\partial x}=2\frac{\partial K_x}{\partial y}\quad ;\quad \frac{\partial^2 \gamma_{yz}}{\partial x\partial y}-\frac{\partial^2 \gamma_{xz}}{\partial y^2}+\frac{\partial K_{xy}}{\partial y}=2\frac{\partial K_y}{\partial x} \tag{5}$$

2.3 Constitutive law

In plane state of stress and for isotropic materials, generally accepted as hypothesis for the calculation of thin structures (beams, plates and shells), the stress–strain relationship equations of Reissner-Mindlin theory are given by

$$\begin{Bmatrix} M_x \\ M_y \\ M_{xy} \\ T_x \\ T_y \end{Bmatrix} = \frac{Eh^3}{12(1-\nu^2)}\cdot\begin{bmatrix} 1 & \nu & 0 & 0 & 0 \\ \nu & 1 & 0 & 0 & 0 \\ 0 & 0 & \frac{(1-\nu)}{2} & 0 & 0 \\ 0 & 0 & 0 & \frac{6k}{h^2}(1-\nu) & 0 \\ 0 & 0 & 0 & 0 & \frac{6k}{h^2}(1-\nu) \end{bmatrix}\cdot\begin{Bmatrix} K_x \\ K_y \\ K_{xy} \\ \gamma_{xz} \\ \gamma_{yz} \end{Bmatrix} \tag{6}$$

Where

- M_x, M_y, M_{xy}, T_x and T_y represent the bending and twisting moments, transverse shear forces per unit length, respectively.
- h, the plate thickness.
- k, the 'shear factor' usually taken as k=5/6, except where mentioned.
- E, Young's modulus.
- **ν**, Poisson's ratio.

3. Formulation of the element "*Pep43*"

3.1 Shape function

For rigid body motions, bending curvatures are related to zero

$$\mathrm{K_x}=0;\qquad \mathrm{K_y}=0;\qquad \mathrm{K_{xy}}=0;\qquad \gamma_{xz}=0;\qquad \gamma_{yz}=0; \tag{7}$$

Putting Eq. (7) into Eq. (3) and Eq. (4) and after integration, the displacement fields can be obtained as follows

$$\beta_x=\mathrm{a}_2\qquad \beta_y=\mathrm{a}_3\qquad \mathrm{W}=\mathrm{a}_1-\mathrm{a}_2\mathrm{x}-\mathrm{a}_3 y \tag{8}$$

where a_1 (arrow) of the rigid body along the normal (axis "z"), a_2 and a_3, are parameters

representing rotations θ_x and θ_y of the rigid body about axis "y" and "x" respectively.

Eq. (8) represents the rigid body motions. The new element has four nodes (see Fig. 1): three vertices to which a fourth fictitious node has been added. Each node has three degrees of freedom, so the displacement fields, formulated by the use of the model deformation, have 12 independent constants (a_1, ..., a_{12}). The first three constants (a_1, a_2, a_3) are used in Eq. (8) to represent rigid body motions. The other nines (a_4 to a_{12}) are used for expressing the displacement due to the straining of the element. They are divided into the deformation interpolation functions to satisfy Eq. (5) of the kinematics compatibility for plane elasticity. Thus, the deformation fields for higher modes are derived from Pascal's triangle as follows

$$K_x = a_4 + a_5 y + a_9 \frac{y}{2};\quad K_y = a_6 + a_7 x + a_{10} \frac{x}{2};\quad K_{xy} = a_8 + a_9 x + a_{10} y;$$

$$\gamma_{xz} = a_{11} - a_7 y^2;\quad \gamma_{yz} = a_{12} - a_5 x^2 \tag{9}$$

Putting Eq. (9) into Eq. (3) and Eq. (4) and after integration, we obtain the displacements fields which are as follows

$$\begin{aligned}
W &= -a_4 \frac{x^2}{2} - a_5 \frac{x^2 y}{2} - a_6 \frac{y^2}{2} - a_7 \frac{xy^2}{2} - a_8 \frac{xy}{2} - a_9 \frac{x^2 y}{4} - a_{10} \frac{xy^2}{4} - a_{11} \frac{x}{2} - a_{12} \frac{y}{2} \\
\beta_x &= +a_4 x + a_5 xy - a_7 \frac{y^2}{2} + a_8 \frac{y}{2} + a_9 \frac{xy}{2} + a_{10} \frac{y^2}{4} + \frac{a_{11}}{2} \\
\beta_y &= -a_5 \frac{x^2}{2} + a_6 y + a_7 xy + a_8 \frac{x}{2} + a_9 \frac{x^2}{4} + a_{10} \frac{xy}{2} + \frac{a_{12}}{2}
\end{aligned} \tag{10}$$

The final displacements field is obtained by substituting Eq. (8) to Eq. (10)

$$\begin{aligned}
W &= a_1 - a_2 x - a_3 y - a_4 \frac{x^2}{2} - a_5 \frac{x^2 y}{2} - a_6 \frac{y^2}{2} - a_7 \frac{xy^2}{2} - a_8 \frac{xy}{2} - a_9 \frac{x^2 y}{4} - a_{10} \frac{xy^2}{4} - a_{11} \frac{x}{2} - a_{12} \frac{y}{2} \\
\beta_x &= a_2 + a_4 x + a_5 xy - a_7 \frac{y^2}{2} + a_8 \frac{y}{2} + a_9 \frac{xy}{2} + a_{10} \frac{y^2}{4} + \frac{a_{11}}{2} \\
\beta_y &= a_3 - a_5 \frac{x^2}{2} + a_6 y + a_7 xy + a_8 \frac{x}{2} + a_9 \frac{x^2}{4} + a_{10} \frac{xy}{2} + \frac{a_{12}}{2}
\end{aligned} \tag{11}$$

The displacement field given by Eq. (11) can be in a matrix form as follows

$$\begin{Bmatrix} W(x, y) \\ \beta_x(x, y) \\ \beta_y(x, y) \end{Bmatrix} = [f(x, y)]\{a_i\} \tag{12}$$

with, $\{a_i\}^T = \langle a_1, a_2, a_3, a_4, a_5, a_6, a_7, a_8, a_9, a_{10}, a_{11}, a_{12} \rangle$

$$[f(x, y)] = \begin{bmatrix} 1 & -x & -y & -\frac{x^2}{2} & -\frac{x^2 y}{2} & -\frac{y^2}{2} & -\frac{xy^2}{2} & -\frac{xy}{2} & -\frac{x^2 y}{4} & -\frac{xy^2}{4} & -\frac{x}{2} & -\frac{y}{2} \\ 0 & 1 & 0 & x & xy & 0 & -\frac{y^2}{2} & \frac{y}{2} & \frac{xy}{2} & \frac{y^2}{4} & \frac{1}{2} & 0 \\ 0 & 0 & 1 & 0 & -\frac{x^2}{2} & y & xy & \frac{x}{2} & \frac{x^2}{4} & \frac{xy}{2} & 0 & \frac{1}{2} \end{bmatrix} \tag{13}$$

Knowing the nodal coordinates (x_i, y_i) corresponding to the nodes j (j = 1... 4) and applying the Eq. (12), the nodal displacements vector at the elementary level is given as follows

$$\{q^e\} = \begin{Bmatrix} [f(x_1, y_1)] \\ [f(x_2, y_2)] \\ [f(x_3, y_3)] \\ [f(x_4, y_4)] \end{Bmatrix} . \{a_i\} \tag{14}$$

with, $\{q^e\}^T = \langle W_1, \beta_{x1}, \beta_{y1}, W_2, \beta_{x2}, \beta_{y2}, W_3, \beta_{x3}, \beta_{y3}, W_4, \beta_{x4}, \beta_{y4} \rangle$

$[A] = \begin{Bmatrix} [f(x_1, y_1)] \\ [f(x_2, y_2)] \\ [f(x_3, y_3)] \\ [f(x_4, y_4)] \end{Bmatrix}$ is the nodal coordinate's matrix. The development of this matrix is shown in the appendix.

From Eq. (14), the value of parameters "a_i" can be deduced and are given by

$$\{a_i\} = [A]^{-1} \{q^e\} \tag{15}$$

Substituting Eq. (15) in Eq. (12), we obtain the following relationship

$$\begin{Bmatrix} W(x, y) \\ \beta_x(x, y) \\ \beta_y(x, y) \end{Bmatrix} = [f(x, y)].[A]^{-1}.\{q^e\} \tag{16}$$

$[N] = [f(x, y)].[A]^{-1}$ represent the matrix of interpolation functions Ni.

Putting Eq. (12) in Eq. (3) and Eq. (4), the relationship strain-displacement takes the following expanded form

$$\begin{Bmatrix} K_x \\ K_y \\ K_{xy} \\ \gamma_{xz} \\ \gamma_{yz} \end{Bmatrix} = \begin{bmatrix} 0 & 0 & 0 & 1 & y & 0 & 0 & 0 & \frac{y}{2} & 0 & 0 & 0 \\ 0 & 0 & 0 & 0 & 0 & 1 & x & 0 & 0 & \frac{x}{2} & 0 & 0 \\ 0 & 0 & 0 & 0 & 0 & 0 & 0 & 1 & x & y & 0 & 0 \\ 0 & 0 & 0 & 0 & 0 & 0 & -y^2 & 0 & 0 & 0 & 1 & 0 \\ 0 & 0 & 0 & 0 & -x^2 & 0 & 0 & 0 & 0 & 0 & 0 & 1 \end{bmatrix} \{a_i\} = [Q(x, y)]\{a_i\} \tag{17}$$

Thus, the deformation matrix [$Q(x, y)$] is given as follows

$$[Q(x, y)] = \begin{bmatrix} 0 & 0 & 0 & 1 & y & 0 & 0 & 0 & \frac{y}{2} & 0 & 0 & 0 \\ 0 & 0 & 0 & 0 & 0 & 1 & x & 0 & 0 & \frac{x}{2} & 0 & 0 \\ 0 & 0 & 0 & 0 & 0 & 0 & 0 & 1 & x & y & 0 & 0 \\ 0 & 0 & 0 & 0 & 0 & 0 & -y^2 & 0 & 0 & 0 & 1 & 0 \\ 0 & 0 & 0 & 0 & -x^2 & 0 & 0 & 0 & 0 & 0 & 0 & 1 \end{bmatrix} \tag{18}$$

3.2 Elementary stiffness matrix

The internal virtual work for an elementary discredited element is given by the expression

$$(\delta W_{int})^e = \int_{V^e} \delta\{\varepsilon\}^T [\sigma] dv^e \tag{19}$$

Knowing that

$$\{\varepsilon\} = [N'] \{q^e\} = [Q(x, y)][A]^{-1} \{q^e\} \tag{20}$$

And

$$\{\sigma\} = [D]\{\varepsilon\} \tag{21}$$

and replacing in the Eq. (19) $\{\varepsilon\}$ and $\{\sigma\}$ by values given respectively in Eqs. (20) and (21) yields

$$(\delta W_{int})^e = \delta\{q^e\}^T \int_{V^e} [Q(x, y)]^T .[A^{-1}]^T .[D][Q(x, y)][A^{-1}]\{q^e\} dv^e \tag{22}$$

Thus, the elementary stiffness matrix derived from the expression (22) is as follows

$$[K^e] = \int_{V^e} [Q(x, y)]^T .[A^{-1}]^T .[D][Q(x, y)][A^{-1}] dv^e \tag{23}$$

The Eq. (23) can be written

$$[K^e] = [A^{-1}]^T \int_{V^e} [Q(x, y)]^T .[D][Q(x, y)] dv^e [A^{-1}] = [A^{-1}]^T .[K_0][A^{-1}] \tag{24}$$

The evaluation of the expression $[K_0]$ is determined by analytic integration of the various components of the resulting matrix product $[Q(x, y)]^T .[D][Q(x, y)]$ whose expressions take the form $H_{\alpha\beta} = C..x^{\alpha}.y^{\beta}$. So the matrix $[K_o]$ is evaluated by analytical integration of values $\int\int_{x\ y} H_{\alpha\beta} = \int\int_{x\ y} C..x^{\alpha}.y^{\beta}$.

Finally, the elementary stiffness matrix, to be considered at the assembly and construction of the global stiffness matrix of the structure, is obtained after condensation of the matrix $[K^e]$. The static condensation is related to the degree of freedom of the fictitious fourth node.

4. Validation of the element *«Pep43»*

4.1 Patch-tests

4.1.1 Rigid modes

This test is performed on one single element. The main objective of this test is to check the representation of rigid body motions i.e., if a displacement field non-zero produces zero strain. To do this, three displacement vectors corresponding to each the rigid modes respectively were defined

- $\{U_{ti}\}$ = {1 0 0; 1 0 0; 1 0 0} for *translation rigid mode,*
- $\{U_{xzi}\}$ = {-x_1 1 0; -x_2 1 0; -x_3 1 0 for *rotation rigid mode « xz »,*
- $\{U_{yzi}\}$ = {-y_1 0 1 ; -y_2 0 1 ; -y_3 0 1} for *rotation rigid mode « yz ».*

Then we verify for each of the above defined vectors the following equation

$$[K]\{U_i\} = \{0\} \tag{25}$$

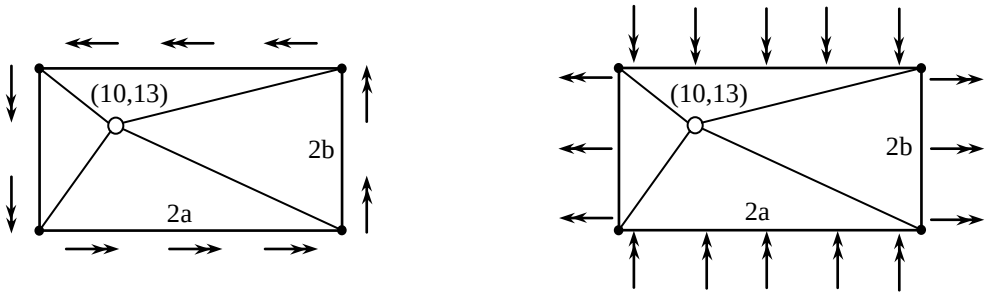

(a) Stresses defined by $\overline{M}_n = 1$ (b) Stresses defined by $\overline{M}_{ns} = 1$

Fig. 2 Stresses on the contour reflecting the constant stress state

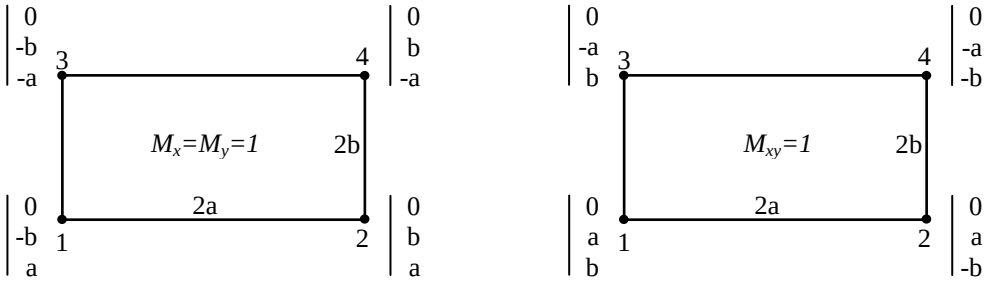

(a) First test (b) Second test

Fig. 3 Equivalents node's forces

The results show that for this element there is a good representation of rigid body motions, since the above condition is satisfied whatever the geometry of the element.

4.1.2 Mechanic patch-test

In this test, an assembly of four triangular elements on a rectangular domain having sides of 2*a*=40 units and 2*b*=20 units. We impose on the contour of this domain stresses reflecting the state of the constant moments (or stresses).

In the first test, stresses on the contour are in agreement with the field defined by $\overline{M}_n = 1$ (See Fig. 2(a)) in order to have $\overline{M}_x = \overline{M}_y = 1$ throughout (See Fig. 3(a)).

In the second test, stresses on the contour are in agreement with the field defined by $\overline{M}_{ns} = 1$ (See Fig. 2(b)) in order to have $\overline{M}_{xy} = 1$ throughout (See Fig. 3(b)). These tests were made for thicknesses varying from 0.01 to 4.0 units.

The other data are defined as follows: E=1000; v=0.3; h=0.01–0.04–1.0– 4.0; $W_1=W_2=W_3=0$

After calculating the elementary stiffness matrix, assembly, taking into accounts the boundary conditions and resolution, the results (nodes 5) are given in Table 1.

From these results it can be concluded that the element passes with success this patch test.

4.2 Cantilever beam subjected to point load at its free end

This test checks the behaviour of the element in simple bending element based on the slenderness ratio (*L/h*). At the free end, the beam is subjected in the direction "*Oz*" to *A* point load of intensity *P = 0.1*.

The other end is simulated as a perfect fitting (see Fig. 4).

The geometrical, mechanical and loading data are given in Table 2.

To see the influence of transverse shear on the behaviour of this new element, in this test case, the displacement "*w*" from point "*A*" in the direction of "*Oz*" for several values of the ratio *L/h* is simulated. The theoretical solution of the displacement "*w*" from point "*A*" in direction "*Oz*" is given as follows, with *k* =5/6:

$$w_t = \frac{4Pl^3}{Ebh^3}\left[1+\frac{1}{2k}\left(\frac{h}{l}\right)^2\right] \tag{26}$$

The simulation results point "*A*" in the direction "*Oz*" is given in Table 3 and Fig. 5.

The results obtained (See Table 3.) show the total absence of the transverse shear blocking phenomenon, since the displacement obtained are from the theoretical solutions regardless the slenderness (l/h ratio). It also can be seen from fig. 5 the robustness of the present new element

Table 1 Results of "mechanical" patch test of element Reissner-Mindlin type

Thickness		*h*=0.01	*h*=0.04	*h*=1.0	*h*=4.0
$\overline{M}_x = \overline{M}_y = 1$	$M_{x(node\ 05)}$	-1	-1	-1	-1
	$M_{y(node\ 05)}$	1	1	1	1
$\overline{M}_{xy} = 1$	$M_{xy(node\ 05)}$	-1	-1	-1	-1

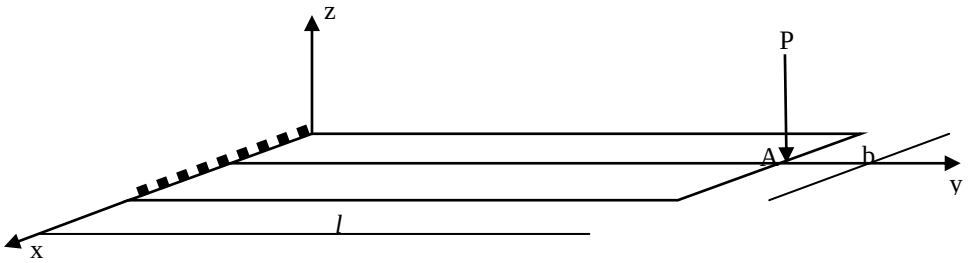

Fig. 4 Cantilever beam subjected to point load

Table 2 Data for the cantilever beam in simple bending

Length	*L*=10 m
Width	*b*=1 m
Thickness	*h*=0.1 to 10m
Young's Modulus	$E=1.2\times10^6$N/m²
Poisson Coefficient	*v*=0
Loading	*P*=0.1 N

Table 3 Displacement from point *A* along the axis "*Oz*" of the cantilever beams in simple bending

L/h	DSTM	ANST6	DKTM	**Pep43**	Theoretical Solution
1	5.1×10^{-7}	5.3×10^{-7}	3.1×10^{-7}	$\mathbf{5.30\times10^{-7}}$	$\mathbf{5.3\times10^{-7}}$
2	2.9×10^{-6}	3.0×10^{-6}	2.5×10^{-6}	$\mathbf{3.05\times10^{-6}}$	$\mathbf{3.1\times10^{-6}}$
3	9.0×10^{-6}	9.6×10^{-6}	8.4×10^{-6}	$\mathbf{9.53\times10^{-6}}$	$\mathbf{9.6\times10^{-6}}$
4	2.0×10^{-5}	2.2×10^{-5}	2.0×10^{-5}	$\mathbf{2.19\times10^{-5}}$	$\mathbf{2.2\times10^{-5}}$
5	4.0×10^{-5}	4.2×10^{-5}	3.9×10^{-5}	$\mathbf{4.23\times10^{-5}}$	$\mathbf{4.3\times10^{-5}}$
10	-	-	-	$\mathbf{3.3\times10^{-4}}$	$\mathbf{3.3\times10^{-4}}$
100	0.31329	-	0.31327	**0.3300**	**0.3333**

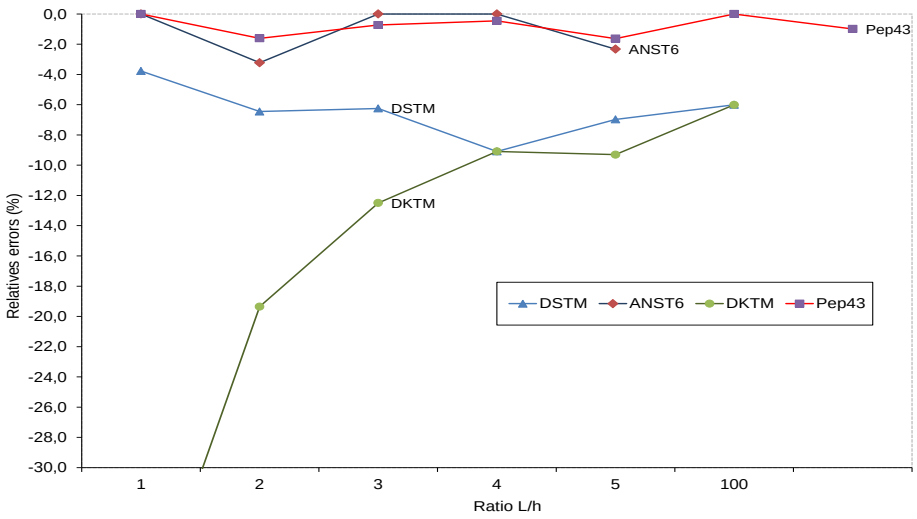

Fig. 5 Relative errors of displacement "*W*" on point A in pure bending

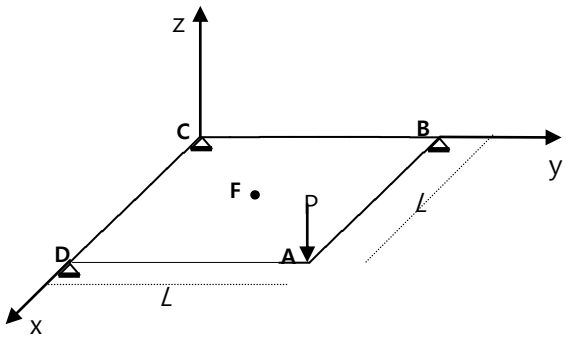

Fig. 6 Twisting of square plate

when compared to the existing elements in the literature. It should be noted that its convergence towards the solution is obtained with a meshing of twenty (20) elements.

4.3 Twisting of a square plate

The plate in Fig. 6 is simply supported (W=0) at the corners B, C and D. A transverse force is applied at corner A.

The geometrical, mechanical and loading data are given in Table 4.

This problem was treated by Batoz *et al.* (1980), Clough and Tocher (1965), and Teodorecu (1982) in order to analyze other finite elements, is considered in the bearing evaluation of the new element in a constant twisting state. The exact solution obtained by the plate theory (thin theory) is given below

W_A (corner A)	0.2496
W_F (centre of plate F)	0.0624
M_X (throughout)	0.0
M_Y (throughout)	0.0
M_{XY} (centre of plate F)	2.5

The displacement results and the moments obtained in the case of the new element Pep43, are compared to other author's elements are given in Table 5.

In this test, the results obtained with k=10^5, show that the new element is robust.

4.4 Isotropic square plate

This example was taken by many authors in the literature including (Batoz *et al.* 1990).

This is an isotropic square plate of side a and thickness h. In this work several scenarios based on the boundary conditions of the plate and the type of loading were simulated. It is a question of studying the behaviour of the present new element, with different mesh sizes and a/h ratios. The displacements obtained at the plate center (Point C) are compared with the references solutions, as shown in tables 6-7-8-9.The trends of convergence are illustrated for various scenarios in the figs 8- 9-10-11.

Table 4 Data for a twisted square plate

Side length	L= 8.0
Thickness	h= 1.0
Young's Modulus	E=10000
Poisson Coefficient	v = 0.3
Loading	P= 5

Table 5 Simulation results of twisting of square plate

Element type	Deflection "W" at		Moments	
	Point A	Point F	M_X et M_Y	M_{XY}
Pep43 (2×2)	**0.24960**	**0.06240**	**0.0**	**2.5**
SBRP (2×2)	0.24960	0.06240	0.0	2.5
DKT	0.24960	0.06240	0.0	2.5
HSM	0.24960	0.06240	0.0	2.5
HCT (8×8)	0.25002	0.06254	0.0	2.5
ACM (8×8)	0.24972	0.06244	0.0	2.5
Exact Solution (Thin theory)	**0.24960**	**0.06240**	**0.0**	**2.5**

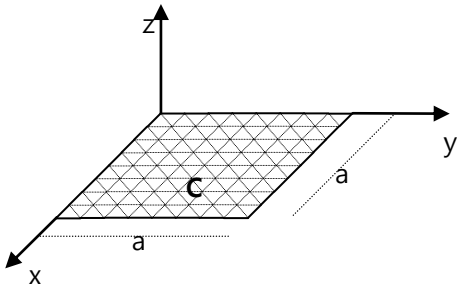

Fig. 7 Isotropic square plate

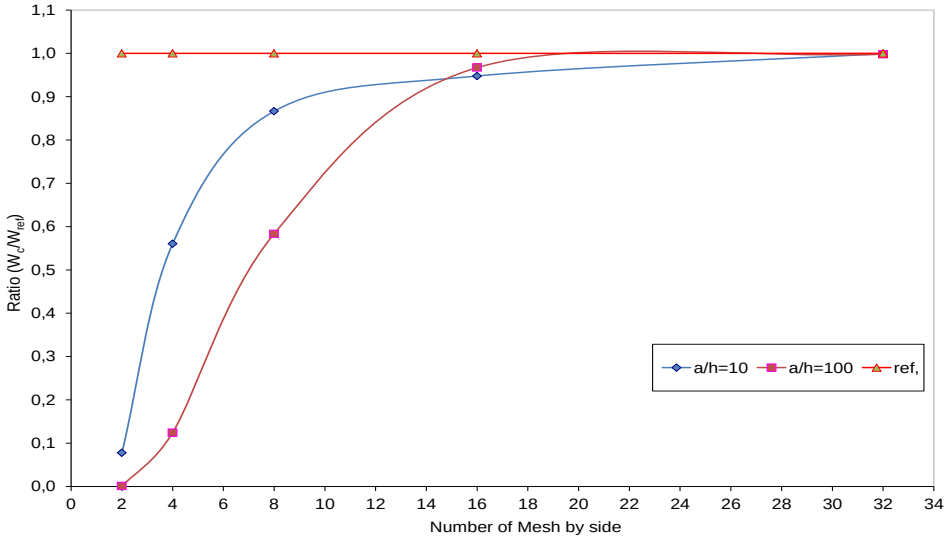

Fig. 8 Ratio of displacement "$W_c/W_{ref.}$" on point *C* - isotropic square plate, simply supported on all four sides

4.4.1 Isotropic square plate requested by a uniformly distributed load

Table 6 displacement (= 100WD/qa^4) on point *C* isotropic square plates, simply supported on all four sides, with $D=Eh^3/12(1-\nu^2)$

	a/h=10				*a/h*=100			
	R4	SBRP	SBH8	Pep43	R4	SBRP	SBH8	Pep43
2×2	0.23169	0.35869	0.35935	0.03583	0.00446	0.06733	0.08817	0.0004
4×4	0.36519	0.43106	0.43161	0.25869	0.01727	0.31151	0.31235	0.0505
8×8	0.43142	0.45245	0.45299	0.40000	0.06128	0.39616	0.39628	0.2369
16×16	-	-	-	0.43752	-	-	-	0.3928
32×32	-	-	-	**0.46137**	-	-	-	**0.4054**
ref		**0.46169**				**0.4062**		

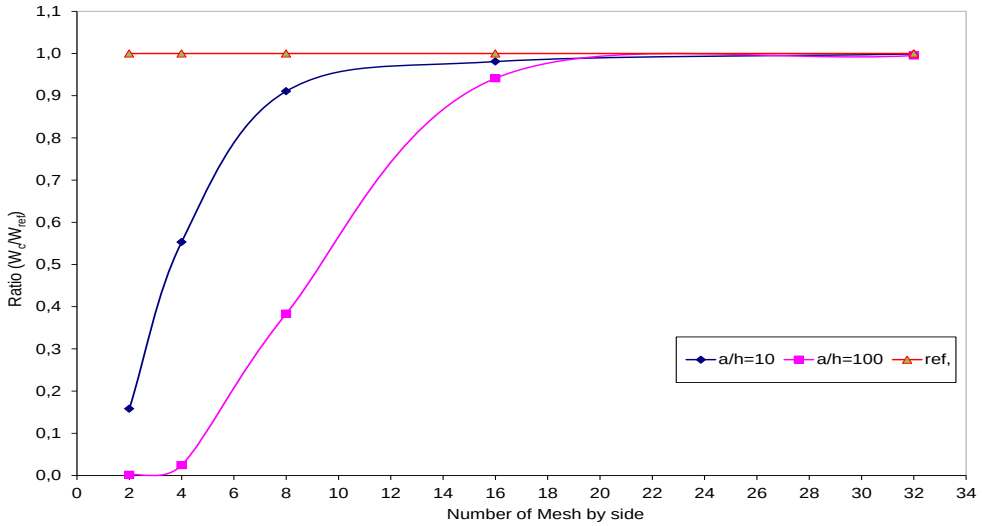

Fig. 9 Ratio of displacement "W_c/W_{ref}" on point *C* - isotropic square plate clamped at its four sides

Table 7 Displacement (= 100WD/qa^4) on point *C* isotropic square plates, clamped at its four sides, with $D=Eh^3/12(1-\nu^2)$

	a/*h*=10				*a*/*h*=100			
	R4	SBRP	SBH8	Pep43	R4	SBRP	SBH8	Pep43
2×2	0.06989	0.09032	0.09089	0.02377	0.00101	0.00270	0.00273	0.0002
4×4	0.11518	0.13836	0.13871	0.08323	0.00367	0.05584	0.056235	0.0031
8×8	0.13954	0.14757	0.14789	0.13700	0.01322	0.11789	0.11797	0.0483
16×16	-	-	-	0.14758	-	-	-	0.1186
32×32	-	-	-	**0.15030**	-	-	-	**0.1254**
Ref.		**0.15046**				**0.126**		

4.4.2 Isotropic square plate requested by a point load applied at its center

Table 8 Displacement (= 100WD/Pa^2) on point *C* isotropic square plates, simply supported on all four sides, with $D=Eh^3/12(1-\nu^2)$

	a/*h*=10				*a*/*h*=100			
	R4	SBRP	SBH8	Pep43	R4	SBRP	SBH8	Pep43
2×2	0.73584	1.06060	1.06336	0.143308	0.01342	0.18284	0.25566	0.001504
4×4	1.12951	1.29855	1.30142	0.803125	0.04846	0.84496	0.85630	0.193668
8×8	1.34606	1.39877	1.40198	1.213846	0.16901	1.11641	1.11674	0.716010
16×16	-	-	-	1.312500	-	-	-	1.085048
32×32	-	-	-	**1.414375**	-	-	-	**1.111154**
ref		**1.44267**				**1.16**		

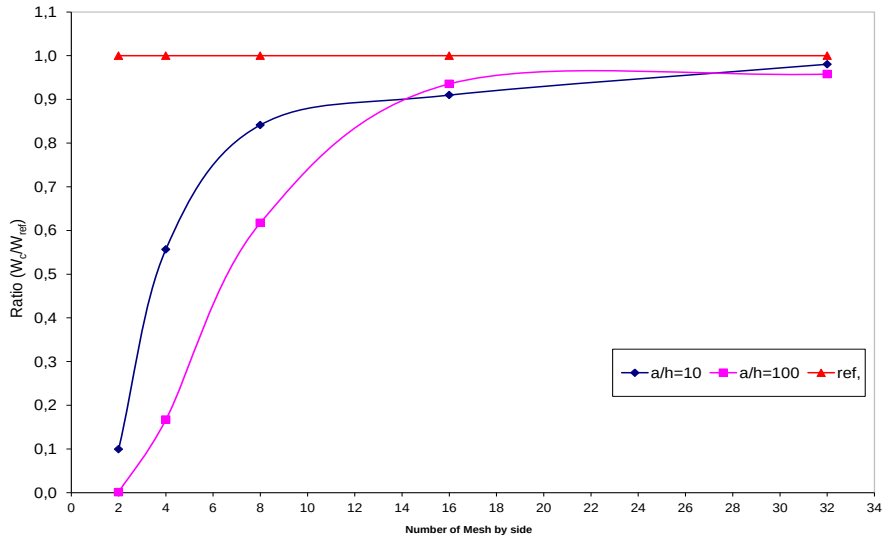

Fig. 10 Ratio of displacement "$W_c/W_{ref.}$" on point *C* - isotropic square plate, simply supported on all four sides

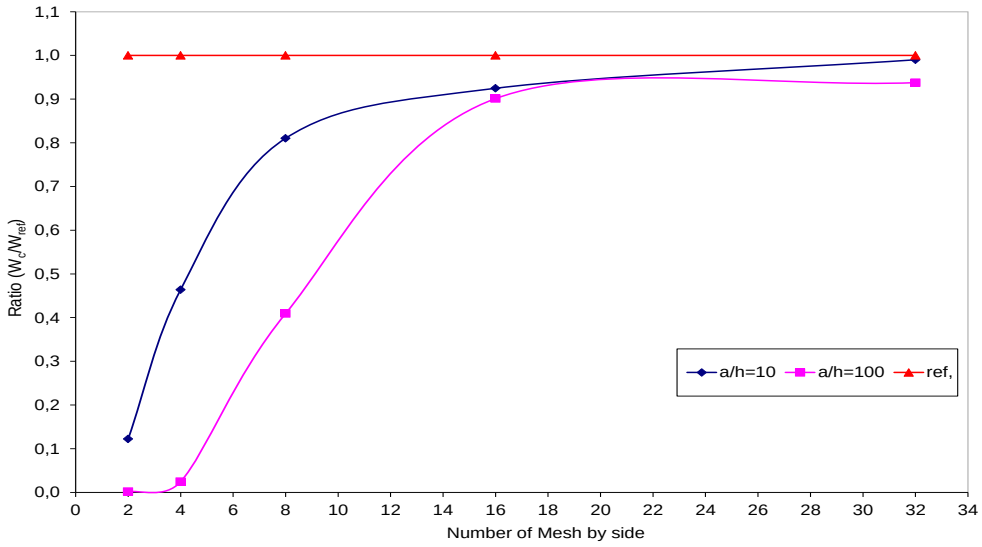

Fig. 11 Ratio of displacement "$W_c/W_{ref.}$" on point *C* - isotropic square plate clamped at its four sides

4.5 Circular plate

This example was used by many authors in the literature including (Batoz *et al.* 1990). In this work several scenarios based on the boundary conditions of the plate under uniform loading *f*, were simulated. In this study, we have considered three meshing, i.e., 4, 16 and 58 (Fig. 12). Each circular plates have a radius $r = 5$ and a thickness $h = 0.5$, *a Poisson's coefficient* $v = 0.36$.

The displacements obtained at the center of the plate (Point *C*) were compared with the

Table 9 Displacement (= 100WD/Pa^2) on point *C* isotropic square plates, clamped at its four sides, with $D=Eh^3/12(1-\nu^2)$

	a/*h*=10				*a*/*h*=100			
	R4	SBRP	SBH8	Pep43	R4	SBRP	SBH8	Pep43
2×2	0.32949	0.39200	0.39486	0.095096	0.00458	0.01064	0.01078	0.000951
4×4	0.57104	0.65236	0.65482	0.360851	0.01690	0.24039	0.24204	0.013793
8×8	0.71499	0.74211	0.74492	0.630240	0.06043	0.51183	0.51216	0.229216
16×16	-	-	-	0.719231	-	-	-	0.504663
32×32	-	-	-	**0.806587**	-	-	-	**0.525096**
Ref.		**0.77775**				**0.56**		

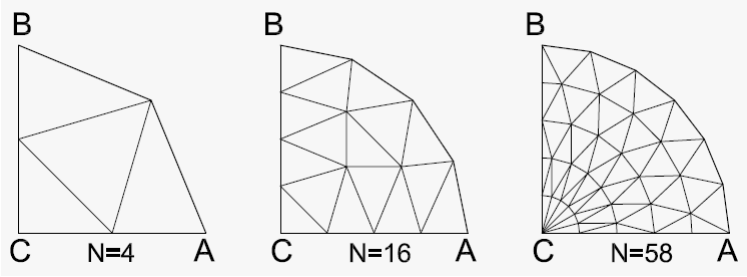

Fig. 12 Circular plate

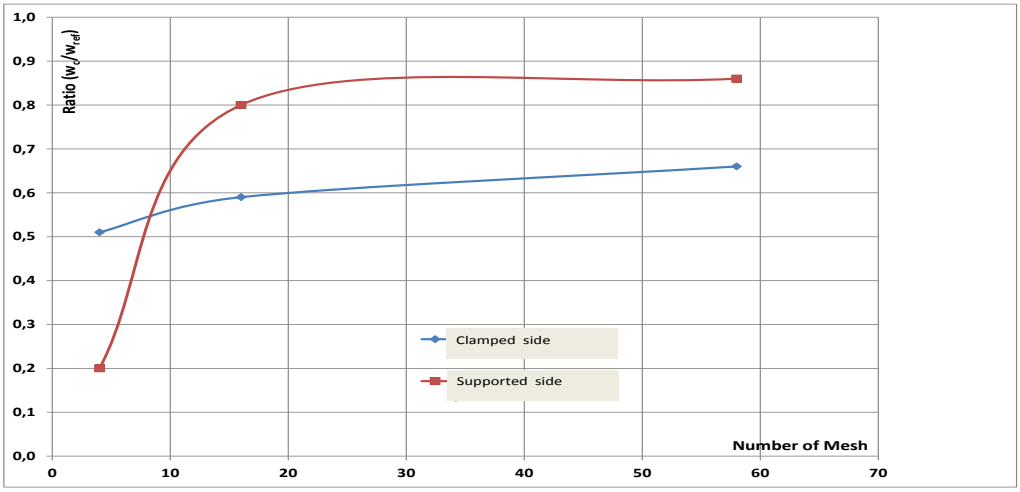

Fig. 13 Ratio of displacement "W_c/W_{ref}." on point *C* - circular plate

reference solutions (Batoz *et al.* 1990). In this case, a ratio (w_c/w_{ref}) was used as a comparison criterion.

Trends of convergence are illustrated for clamped and supported side in Fig. 13.

For supported plate, the reference solution is

$$w_{ref} = \frac{f.r^4}{64D}\left(\frac{5+\nu}{1+\nu}+\phi\right) \tag{27}$$

For clamped plate, the reference solution is

$$w_{ref} = \frac{f.r^4}{64D}(1+\phi) \tag{28}$$

With $\phi = \frac{16}{5}\left(\frac{h}{r}\right)^2 \frac{1}{1-\nu}$ and $D = \frac{Eh^3}{12(1-\nu^2)}$

5. Conclusions

In this work, we have presented a new triangular bending finite element in the perspective of linear static and dynamic analysis, also for the geometric non linear of curved structures (arch and shell) analysis. The adopted approach and the development of concepts and techniques used have allowed coming to a competitive, robust and efficient finite element for the treatment of thin and thick plates. It is an element which shows undoubted advantages which plead to its use. The presence of the fictitious node and the adoption of the "deformation" approach have given the opportunity of enriching the displacement fields, and consequently, a greater accuracy in the approximation of the solution by avoiding the complexity of the classical theories. The reduction of elementary stiffness matrices by the means of the "static condensation" technique, action related to the degrees of freedom of the fictitious node, by which solving enormous systems of equations can be avoided, therefore, non negligible savings of time are recorded. The use of analytical integration in the evaluation of the stiffness matrix, gave this new element a competitive behaviour. These results were remarkable in the convergence tests carried out where a rapid trend towards the solution on the contrary to the isoperimetric elements (using numerical integration) have been noticed. Furthermore, our element has passed successfully the patch-tests related to the constant deformations state (stiff modes and constant modes). Besides, it was noticed a lack of the blocking connected to the transverse shear.

References

Argyris, J.H., Dune, P.C., Malejannakis, G.A. and Schelkle, E. (1977), "A simple triangular facet shell element with applications to linear and non linear equilibrium and elastic stability problems", *Comput. Method. Appl. Mech. Eng.*, **10**(3), 371-403.

Barik, M. and Mukhopadhyay, M. (2002), "A new stiffened plate element for the analysis of arbitrary plates", *Thin Wall. Struct.*, **40**(7-8), 625-639.

Batoz, J.L., Bath, K.J. and Ho, L.W. (1980), "A study of three nodes triangular plate bending elements", *Int. J. Numer. Meth. Eng.*, **15**, 1771-812.

Batoz, J.L. and Dhatt, G. (1990), *Modélisation des structures par éléments finis, Vol.1, Solides Elastiques, Vol 2 : Poutres et plaques*, Hermes, Paris.

Belarbi, M.T. and Charif, A. (1999), "Développement d'un nouvel élément hexaédrique simple basé sur le modèle en déformation pour l'étude des plaques minces et épaisses", *Revue Européenne des Éléments Finis*, 135-157.

Belounar, L. and Guenfoud, M. (2005), "A new rectangular finite element based on the strain approach for plate bending", *Thin Wall. Struct.*, **43**, 47-63.

Belytschko, T., Ong, J.S.J., Liu, W.K. and Kennedy, J.M. (1984), "Hourglass control in linear and nonlinear

problems", *Compute Method. Appl. Mech. Eng.*, **43**, 251-276.
Brasile, S. (2008), "An isostatic assumed stress triangular element for the Reissner-Mindlin plate bending problem", *Int. J. Numer. Meth. Eng*., **74**, 971-995.
Chinosi, C. (2005), "PSRI elements for the Reissner–Mindlin free plate", *Comput. Struct.*, **83** (31-32), 559-2572.
Clough, R.W. and Tocher, J.L. (1965), "Finite element stiffness matrixes for analysis of plate bending", *Proceeding of first conference Matrix methods in structural mechanics, Wright-Patterson Air force baseman*, Ohio.
Boutagouga, D., Gouasmia, A. and Djeghaba, K. (2010), "Geometrically non-linear analysis of thin shell by a quadrilateral finite element with in-lane rotational degrees of freedom", *European Journal of Computational Mechanics/Revue Européenne de Mécanique Numérique*, **19 (**8), 707-724.
Kim, D.N. and Bathe, K.J. (2009), "A triangular six-node shell element", *Comput. Struct.*, **87**(23-24), 1451-1460.
Frey, F. (1998), "*Traité de génie civil de l'école polytechnique fédérale de Lausane*", *Volume 3, Analyse des structures et milieux continus - mécanique des solides*, Presses polytechniques et universitaires romandes CH-1015.
Guenfoud, M. (1990), "Deux éléments triangulaires nouveaux pour l'analyse linéaire et non linéaire géométrique des coques", Thèse de doctorat, Institut national des sciences appliquées de Lyon, France
Hamadi, D.J. and Belarbi, M.T. (2006), "Integration solution routine to evaluate the element stiffness matrix for distorted shape", *Asian J. Civil Eng*., 7(5), 525-549.
Han, S.C., Ham, H.D. and Nuklchaic, W.K. (2008), "Geometrically non-linear analysis of arbitrary elastic supported plates and shells using an element-based Lagrangian shell element", *Int. J. Nonlin. Mech.*, **43**, 53-64.
Himeur, M. (2008), "Développement d'éléments membranaires nouveaux d'élasticité plane basés sur la formulation en déformation", Thèse de magistère, Université de Guelma (Algérie), Département de Génie Civil, 104p
Himeur, M. and Guenfoud, M. (2011), "Bending triangular finite element with a fictitious fourth node based on the strain approach", *European Journal of Computational Mechanics/Revue Européenne de Mécanique Numérique*, **20(**7-8), 455-485.
Maalem, T. (2007), "Contribution au modèle en déformation dans l'analyse des structures", Thèse de Doctorat, Université de Batna (Algérie).
Man, H., Song, C., Xiang, T., Gao, W. and Tin-Loi, F. (2013), "High-order plate bending based on the boundary finite element method", *Int. J. Numer. Meth. Eng.*, **95**, 331-360.
Providas, E. and Kattis, M.A. (2000), "An assessment of two fundamental flat triangular shell elements with drilling rotation", *Comput. Struct.*, **77**, 129-139.
Sabourin, F.M. and Salle, F. (2000), "Calcul des structures par éléments finis, Barres" - Poutres Elasticité plane Axisymétrique Plaques - coques non linéarité", Chapitre IV, INSA Lyon, France.
Yuan, F. and Miller, R.E. (1988), "A rectangular finite element for moderately thick flat plate", *Comput. Struct*., **30**, 1375-87.

Appendix A.

Formulation of the matrix of rigidity at the elementary level

$$[K_0]=\frac{Eh^3}{12(1-\nu^2)}\iint\begin{bmatrix}0&0&0&0&0\\0&0&0&0&0\\0&0&0&0&0\\1&0&0&0&0\\y&0&0&0&-x^2\\0&1&0&0&0\\0&x&0&-y^2&0\\\frac{y}{2}&0&1&0&0\\0&0&x&0&0\\0&\frac{x}{2}&y&0&0\\0&0&0&1&0\\0&0&0&0&1\end{bmatrix}\cdot\begin{bmatrix}1&\nu&0&0&0\\\nu&1&0&0&0\\0&0&\frac{(1-\nu)}{2}&0&0\\0&0&0&\frac{6k}{h^2}(1-\nu)&0\\0&0&0&0&\frac{6k}{h^2}(1-\nu)\end{bmatrix}\cdot\begin{bmatrix}0&0&0&1&y&0&0&\frac{y}{2}&0&0&0&0\\0&0&0&0&0&1&x&0&0&\frac{x}{2}&0&0\\0&0&0&0&0&0&0&1&x&y&0&0\\0&0&0&0&0&0&-y^2&0&0&0&1&0\\0&0&0&0&-x^2&0&0&0&0&0&0&1\end{bmatrix}dx.dy$$

Appendix B.

Nodal Coordinate Matrix [A]

$$[A]=\begin{bmatrix}1&-x_1&-y_1&-\frac{x_1^2}{2}&-\frac{x_1^2y_1}{2}&-\frac{y_1^2}{2}&-\frac{x_1y_1^2}{2}&-\frac{x_1y_1}{2}&-\frac{x_1^2y_1}{4}&-\frac{x_1y_1^2}{4}&-\frac{x_1}{2}&-\frac{y_1}{2}\\0&1&0&x_1&x_1y_1&0&-\frac{y_1^2}{2}&\frac{y_1}{2}&\frac{x_1y_1}{2}&\frac{y_1^2}{4}&\frac{1}{2}&0\\0&0&1&0&-\frac{x_1^2}{2}&y_1&x_1y_1&\frac{x_1}{2}&\frac{x_1^2}{4}&\frac{x_1y_1}{2}&0&\frac{1}{2}\\1&-x_2&-y_2&-\frac{x_2^2}{2}&-\frac{x_2^2y_2}{2}&-\frac{y_2^2}{2}&-\frac{x_2y_2^2}{2}&-\frac{x_2y_2}{2}&-\frac{x_2^2y_2}{4}&-\frac{x_2y_2^2}{4}&-\frac{x_2}{2}&-\frac{y_2}{2}\\0&1&0&x_2&x_2y_2&0&-\frac{y_2^2}{2}&\frac{y_2}{2}&\frac{x_2y_2}{2}&\frac{y_2^2}{4}&\frac{1}{2}&0\\0&0&1&0&-\frac{x_2^2}{2}&y_2&x_2y_2&\frac{x_2}{2}&\frac{x_2^2}{4}&\frac{x_2y_2}{2}&0&\frac{1}{2}\\1&-x_3&-y_3&-\frac{x_3^2}{2}&-\frac{x_3^2y_3}{2}&-\frac{y_3^2}{2}&-\frac{x_3y_3^2}{2}&-\frac{x_3y_3}{2}&-\frac{x_3^2y_3}{4}&-\frac{x_3y_3^2}{4}&-\frac{x_3}{2}&-\frac{y_3}{2}\\0&1&0&x_3&x_3y_3&0&-\frac{y_3^2}{2}&\frac{y_3}{2}&\frac{x_3y_3}{2}&\frac{y_3^2}{4}&\frac{1}{2}&0\\0&0&1&0&-\frac{x_3^2}{2}&y_3&x_3y_3&\frac{x_3}{2}&\frac{x_3^2}{4}&\frac{x_3y_3}{2}&0&\frac{1}{2}\\1&-x_4&-y_4&-\frac{x_4^2}{2}&-\frac{x_4^2y_4}{2}&-\frac{y_4^2}{2}&-\frac{x_4y_4^2}{2}&-\frac{x_4y_4}{2}&-\frac{x_4^2y_4}{4}&-\frac{x_4y_4^2}{4}&-\frac{x_4}{2}&-\frac{y_4}{2}\\0&1&0&x_4&x_4y_4&0&-\frac{y_4^2}{2}&\frac{y_4}{2}&\frac{x_4y_4}{2}&\frac{y_4^2}{4}&\frac{1}{2}&0\\0&0&1&0&-\frac{x_4^2}{2}&y_4&x_4y_4&\frac{x_4}{2}&\frac{x_4^2}{4}&\frac{x_4y_4}{2}&0&\frac{1}{2}\end{bmatrix}$$